

INVESTIGATING THE EFFECTS OF MOISTURE INGRESS ON THE PERFORMANCE AND SERVICE LIFE OF AUSTRALIAN MASS TIMBER PANELS-CHARACTERIZATION OUTCOMES.

Maryam Shirmohammadi¹

ABSTRACT: Composite timber systems made of timber and massive wood products used in construction are susceptible to moisture fluctuations during transport, construction, and post-construction. The wetting dynamics, both ingress and egress, of Australian timber species and mass panels exposed to Australian climate conditions have not been extensively explored. Understanding moisture movement in timber is crucial for predicting the design life of timber products and developing decay modelling protocols. An experimental testing has been conducted in detail to comprehend water movement and moisture gradients in massive wood-based composites. The testing results presented in this paper include the density, porosity, gas, and liquid permeability of three Australian timber species (radiata pine, southern pine and shining gum). The experiments have been designed to explore the hygroscopic properties of timber species in different directions, including face, edge and end and of CLT (2P and 3P) and LVL sections. The porosity values for the three tested species were $56\% \pm 5$, $57\% \pm 3$ and $42\% \pm 8$ for radiata pine, southern pine and shining gum respectively. The experimental results presented in this paper showed that CLT samples made from radiata pine with edge gap (3P) had higher porosity and permeability values than solid radiata sample sections. The CLT 2P sections had lower porosity values than the solid radiata pine samples. The porosity values determined for LVL (made from pine) samples ($51\% \pm 3$) were slightly lower than southern pine samples tested. The outcomes of this project will facilitate the prediction of product response to moisture and enable the development of maintenance protocols and remedial solutions for the industry to minimize the potential impacts of moisture penetration in mass timber products in the future.

KEYWORDS: Mass timber panels, moisture ingress, service life, cross laminated timber, laminated veneer lumber.

1 INTRODUCTION

Timber and composite timber systems as building materials provide significant advantages such as low embodied energy, excellent insulation properties, and cost-effective construction processes. However, they are vulnerable to dimensional instability, aesthetic deterioration, and fungal decay if exposed to moisture for a prolonged period. Additionally, poorly designed or maintained timber products and buildings can be impacted by biodegradation. The extent and rate of damage can vary, depending on the environmental conditions to which the products are exposed [1-8]. Moisture intrusion into solid timber or mass panel composites and cyclic variation in moisture during and post-construction could cause changes in appearance and structural properties that can be difficult and costly to repair. Southern pine (*Pinus elliottii* x *Pinus caribaea*) (SP), radiata pine (*Pinus radiata*) (RP) and shining gum (*Eucalyptus nitens*) (SG) are three commercially available timber species in Australia. Various studies [9-12] have focused on the properties of wood during drying; however, the movement of water in these three species during periodic and long-term wetting when exposed to free water still requires further research. Specifically, the effects of species' anatomical features (cell arrangement

and direction) and variations between solid timber products and engineered wood products (EWPs), on the wetting and drying process need to be investigated [9-12]. The differences between species and the effects of their anatomical characteristics (such as pore size/types, permeability, chemistry and cell size) on moisture movement over time are important when longer-term durability and structural stability of products are estimated [13-17]. The hygroscopic properties of building elements affect the different aspects of building design and performance, including durability, performance and thermal comfort [18-21]. The EWPs' structure specifically the direction of boards/the arrangement of veneers, glue lines, edge gaps and cracks, impact the EWPs' long-term performance in-service [19, 22-26]. Moisture ingress into solid wood and EWPs could occur through different wetting events and due to poor site management during erection, poor building design, types of construction or poor maintenance [27]. In addition to the complexity of moisture ingress and egress scenarios for EWPs, there is also a need for further research relevant to long-term performance aspects of these components when used in the wide variety of Australian environments in which timber is employed (e.g. higher decay hazard situations)

¹Maryam Shirmohammadi, Principal research scientist,
Queensland department of agriculture and fisheries,
Brisbane, Australia,
Maryam.shirmohammadi@daf.qld.gov.au

[28, 29]. This paper discusses porosity, density, and permeability measurements of solid timber (sawn timber) from three Australian species and Australian mass timber panels. The study was conducted as a part of a larger project developing a mathematical model of moisture ingress/egress into EWPs.

2 MATERIALS AND METHODS

2.1 SAMPLES

Kiln-dried boards of radiata pine (*Pinus radiata* D. Don), Caribbean pine/Slash pine hybrid (*Pinus caribaea* Morelet/*P. elliottii* Engelm.), and shining gum (*Eucalyptus nitens* H. Deane & Maiden) were cut into samples oriented to allow moisture movement to be studied in three different directions. Before testing, three-layer radiata pine cross-laminated timber (CLT) and laminated veneer lumber (LVL) were cut into small sections. Figure 1 shows the sample directions, including the end grain orientation (L (longitudinal)/ D3, R (radial)/D1 or T(tangential)/D2) of boards; for CLT samples, directions included face/D1 (radial/tangential), edge/D3 and end/D2. For LVL samples, directions included face/D1 (radial/tangential), edge/D3 (mostly radial) and end/D2 (longitudinal). All samples were conditioned to constant weight (65%RH/25°C) at approximate 12% EMC, and the initial dimensions of each were recorded.

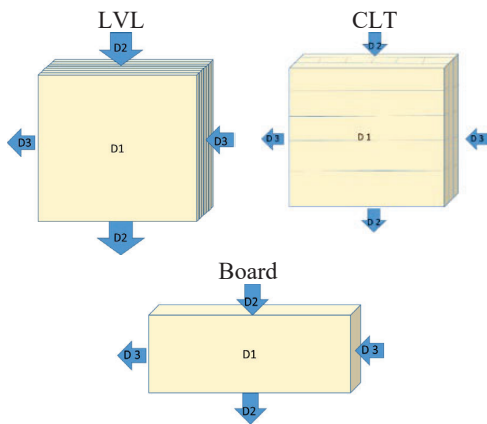


Figure 1: Directions of water movement that were studied.

2.2 DENSITY AND POROSITY

The density porosity of samples was determined for blocks of 20x20x20 mm that were conditioned at 12% EMC before being weighed, and their dimensions were measured to determine the density (Table 1). A helium pycnometer [30] was used to measure the density and porosity of the samples. Five replication of material type was used for the density and porosity measurements.

Table 1: The average sample weights and density used to determine the samples' porosity.

Material Type	Weight (g)	Density (kg/m ³)
Shining gum	4.72 ± 0.2	589.82 ± 32

Radiata pine	4.53 ± 0.2	583.69 ± 58
Southern pine	4.81 ± 0.3	607.45 ± 87
LVL	5.98 ± 0.2	688.65 ± 23
CLT-3P	4.04 ± 0.1	506.13 ± 12
CLT 2p	4.1 ± 0.1	519.20 ± 17

Note: ± are standard deviation values

For CLT and LVL sample types are presented in Figure 2. Apparent density (D_a) in kgm⁻³ using the volume of the piece, including void space, was calculated using Eq. 1. For true density (D_t), the density of samples without voids, samples were placed in a gas pycnometer where density was recorded five times and average values were used for data analysis.

$$D_a = \frac{Mass}{Volume} \quad Eq. 1$$

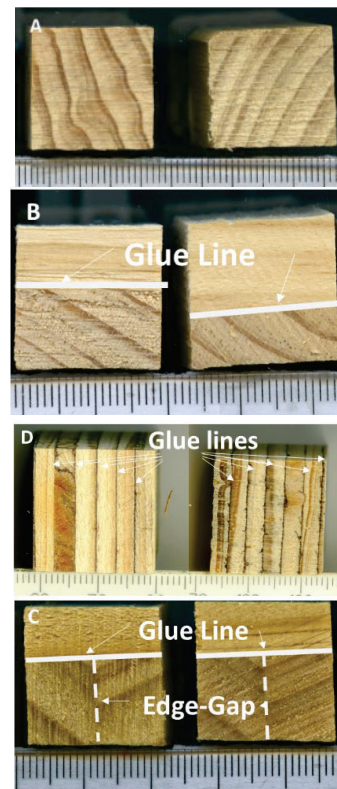


Figure 2: Sample blocks used for porosity and density measurement ((A) solid, (B) CLT-2P (sample with glue line), (C) CLT-3P (sample with glue line and edge gap) and (D) LVL)

The porosity of samples was calculated using the true and apparent density values. The porosity (\emptyset) of samples was calculated using Eq. 2.

$$\emptyset = \left(1 - \left(\frac{D_a}{D_t} \right) \right) \times 100 \quad Eq. 2$$

MICROSCOPIC IMAGING AND CELL DIMENSION MEASUREMENT

In this study, the impact of cell pore size and porosity was evaluated on samples obtained from different surfaces (i.e., face, end, and edge) of a given material. To examine and quantify the cell type and size of the samples, a Nikon ECLIPSE LV100ND/LV100NDA microscope was used, and the images were captured at magnifications of 10x, 20x, and 50x (Figure 3). The average size of the cell lumen was determined for 3-5 anatomical images of each species using ImageJ software [34]. In softwood samples, the size of the cells in earlywood and latewood sections was measured, along with the diameter of resin canals and vessels (Figure 3).

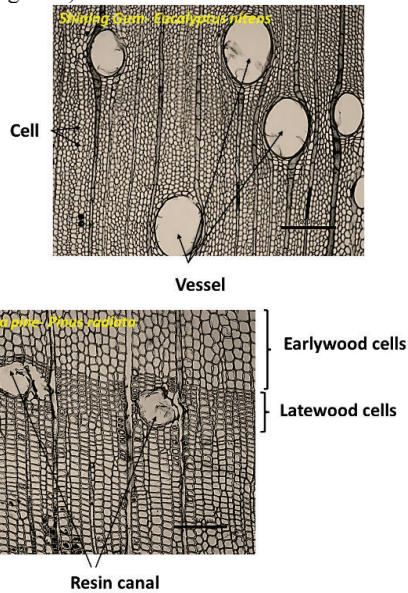


Figure 3: Example images used for determining the cell dimension at 10x magnification [31].

2.3 PERMEABILITY

The gas and liquid permeability of the three solid timber species, CLT and LVL composite panels were determined in the laboratory. Gas permeability was calculated using Darcy's law (Eq. 3) as shown in [15, 32].

$$K = \frac{Q\mu eP}{A\Delta PP} \quad \text{Eq. 3}$$

In this equation, K is the intrinsic permeability (m²); Q is the air flux (m² s⁻¹); μ is the dynamic viscosity of air (Pa); e is the sample thickness (m); P is the pressure at which flux Q is measured (Pa); A is the sample area (m²); ΔP is the pressure difference between the air outlet and inlet sides of the sample (Pa); and \bar{P} is the average pressure inside the sample (Pa). Samples (8-10 mm thick) were cut along the radial, tangential and longitudinal directions using a 24 mm diameter hole-saw. Ten replicates were tested per sample type and direction. Water movement

into the side surfaces of the sample and guarantee air tightness was restricted by the application of two layers of epoxy resin [15].

The effects of glue line and edge gaps were studied for LVL and CLT samples using the sample shown in Figure 4.

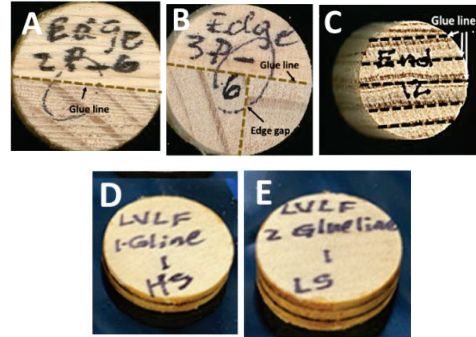


Figure 4: Sample sections (A) CLT (2Piece/2P) (B) CLT (3Piece/3P), (C) LVL (End), (D) LVL (face- one glue line), and (E) LVL (face- two glue lines).

The study tested the permeability of LVL samples with one (4-5 mm thick) and two (7-8 mm thick) glue lines.

3 RESULTS AND DISCUSSION

3.1 POROSITY

The type and size of wood cells influence the hygroscopic properties of products exposed to in-service conditions. Previous research has explored the relationship between pore size and porosity, permeability, and treatability of products, with a focus on natural weathering and water absorption, porosity and sorption isotherm, and capillary condensation in mass timber buildings [33-36].

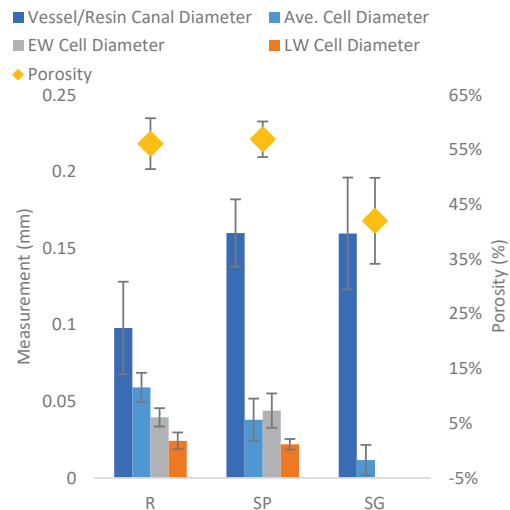


Figure 5: Anatomical features measurements for radiata pine, southern pine, and shining gum samples and calculated porosity. Errors bars represent one standard deviation.

The relationship between the porosity values and anatomical features showed higher cell diameter and porosity values following similar trends (Figure 5). Similarly, previous studies showed higher porosity of timber species linked to lower resistance to moisture flow in the product's structure [30]. The porosity of southern pine samples was higher than that of radiata pine samples, and the anatomical features measured were similar except for a higher resin canal diameter for southern pine samples. Shining gum had lower porosity than the pine samples. A higher percentage of pore in timber product's structure can lead to higher water gain when exposed to moisture [37, 38], so it is important to consider product and species porosity values when modelling wetting and drying processes.

As shown in Figure 5, porosity and true density values were higher for radiata pine and southern pine than for shining gum samples. Southern and radiata pine samples had higher true density than shining gum samples. The bulk densities of all three species were in the sample range (as reported in Table 1).

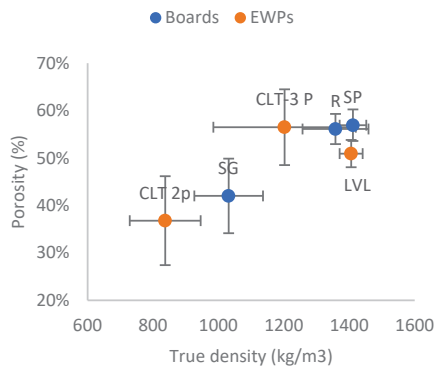


Figure 6: Average porosity versus true density of solid shining gum (SG), radiata pine (R), Caribbean/slash pine (SP) hybrid timbers, radiata pine LVL, or southern pine CLT with 2 or 3 glue lines.

The CLT 3P sections (with glue line and edge gap) showed higher porosity values than CLT 2P (with glue line only) samples. The presence of an edge gap can affect the higher values. The average porosity value for solid radiata pine samples was slightly higher than for CLT 2P. This can result from the glue line in the 2P sample structure. Previously, the effects of cracks and edge gaps in the timber product structure are reported to increase the liquid flow and water trapping into the bulk material. This has been considered a factor affecting the structural and aesthetic performance issues of EWPs if not managed appropriately [39, 40]. The average porosity and density value for LVL samples was lower than the average value for southern pine solid samples.

3.2 PERMEABILITY

As expected, solid wood's gas and liquid permeability results were higher in the longitudinal direction than in the

tangential and radial directions for the three species [14, 15, 41]. Shining gum samples showed higher variability in gas permeability data in the longitudinal direction. The gas permeability values determined for shining gum were close to zero in the radial and tangential directions (Figure 7). Southern pine samples had the highest gas permeability than southern pine and shining gum samples.

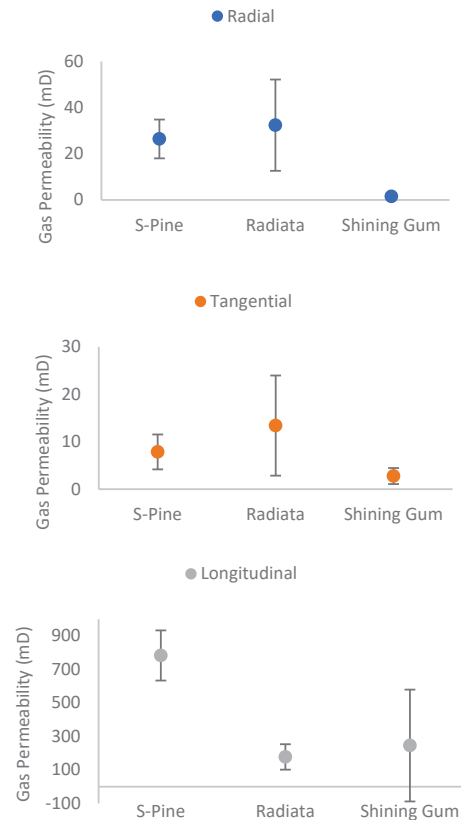


Figure 7: Gas permeability data for species tested, (SP is southern pine, R is radiata pine, SG is shining gum and L, R and T refer to longitudinal, radial and tangential directions).

A higher ratio of gas permeability anisotropy was observed for shining gum in K_L/K_R than radiata or southern pine samples (Table 2). The longitudinal to tangential liquid permeability ratio (K_L/K_T) was much higher for shining gum compared to southern pine and radiata pine. The longitudinal to tangential gas permeability ratio (K_L/K_T) was higher for southern pine and shining gum and lower for radiata pine. These ratios suggest that the pressure required for the movement of liquid and gas in the sample affects the hygroscopic properties of timber boards and composites when exposed to free water. The same process happens when the product is exposed to repeated wetting and drying, which leads to a moisture gradient development inside the product's structure [36]. It is reported that the anisotropic ratios could influence the scale of wetting and drying processes and lead to dimensional changes and internal stresses that are critical factors, especially in CLT connection design

and maintenance [13, 14, 17]. The ratios (K_R/K_T) were much lower for both gas and liquid permeability values in the radial to tangential direction than K_L/K_T and K_L/K_R and shining gum had lower values than the pine samples. The very low permeability caused the high K_L/K_T (ratio of K in longitudinal over tangential directions) value for southern pine in the tangential direction.

Table 2: Anisotropy ratios of sample permeability values determined for solid timber of three species.

Species	Permeability	K_L/K_R	K_L/K_T	K_R/K_T
Southern pine (SP)	Gas	29.65	99.80	3.37
	Liquid	202.66	1396.53	0.00071
Radiata pine (R)	Gas	5.48	13.25	2.42
	Liquid	16.46	233.62	0.0043
Shining gum (SG)	Gas	159.35	88.88	0.56
	Liquid	-	7579	0.00013

± values are the standard deviation.

Figure 8 shows that southern pine samples had a higher liquid permeability in the longitudinal direction when compared to radiata and shining gum samples. Shining gum had the lowest radial and tangential liquid permeability, while radiata pine samples had the lowest longitudinal liquid permeability.



Figure 8: Liquid permeability data for species tested.

The lower permeability rates in shining gum can be attributed to its small cell size arrangement compared to the softwood samples [45]. The other factors, including the extractive and resin content, must be considered when permeability. Southern pine samples had the highest gas permeability compared to other species tested. Southern pine samples also had the highest longitudinal permeability than the other two species.

Figure 9 shows the permeability values determined for CLT 2P and 3P samples. Higher gas and liquid permeability was observed for CLT 3P sections. This result shows the importance of moisture management programs, especially when CLT panels are exposed to weathering, such as flash flooding and heavy rain during construction. The CLT structure and pathways for higher water ingress into the structure (due to edge gaps and cracks) can result in accelerated moisture intrusion leading to more conducive conditions for the fungal attack in the longer term. The LVL gas permeability values determined were 28.8 ± 17 and 20.4 ± 13 mD for samples with one and two glue lines, respectively. The liquid permeabilities were 1.21 ± 1 and 0.63 ± 1 mD for samples with one and two glue lines, respectively.

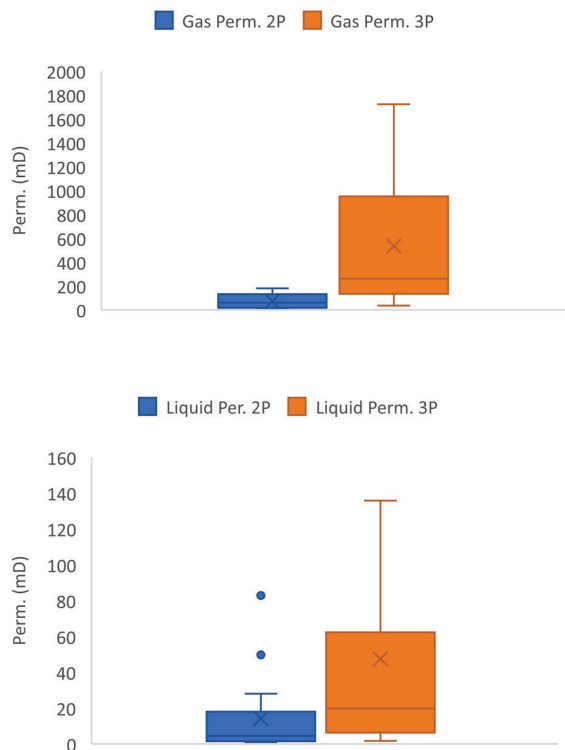


Figure 9: Average gas and liquid permeability values recorded for CLT 2P and 3P sections.

4 CONCLUSIONS

This study determined some hygroscopic properties of Australian timber species and EWP (CLT and LVL) samples. The study focused on determining the porosity, density and permeability properties of the products tested. The determined porosity showed that CLT 2P (sections with glue line) made from radiata pine had lower porosity than the radiata pine samples tested. The CLT section with glue line and edge gaps had higher porosity values than the 2P sections. LVL samples had lower porosity than the radiata and southern pine samples tested. Southern pine samples had higher gas permeability in all directions than radiata pine and shining gum samples. The liquid permeability of southern pine samples was higher in the longitudinal direction than the other two species tested. The observed variations in porosity and permeability values between CLT sections with glue line (2P) and glue line and edge gap (3P) should be considered as potential factors that could affect moisture gain and the development of moisture gradients within the CLT layered structure.

ACKNOWLEDGEMENT

The paper's author would like to acknowledge the National Centre for Timber Durability and Design life

(NCTDDL) for funding this study and the technical team at the Salisbury research facility for assistance during sample preparation and experimental testing.

REFERENCES

- [1] Brischke, C. and G. Alfredsen, *Wood-water relationships and their role for wood susceptibility to fungal decay*. Applied Microbiology and Biotechnology, 2020. **104**(9): p. 3781-3795.
- [2] Isaksson, T., C. Brischke, and S. Thelandersson, *Development of decay performance models for outdoor timber structures*. Materials and Structures, 2013. **46**(7): p. 1209-1225.
- [3] Libralato, M., et al. *Damage risk assessment of building materials with moisture hysteresis*. in *Journal of Physics: Conference Series*. 2021. IOP Publishing.
- [4] Libralato, M., et al. *Multiyear hygrothermal performance simulation of historic building envelopes*. in *IOP Conference Series: Earth and Environmental Science*. 2021. IOP Publishing.
- [5] Libralato, M., et al., *Effects of considering moisture hysteresis on wood decay risk simulations of building envelopes*. Journal of Building Engineering, 2021. **42**: p. 102444.
- [6] Viitanen, H., et al., *Towards modelling of decay risk of wooden materials*. Eur. J. Wood Prod, 2010. **68**: p. 303-313.
- [7] Viitanen, H., *Factors affecting the development of mould and brown rot decay in wooden material and wooden structures: Effect of humidity, temperature and exposure time*. 1998.
- [8] Shirmohammadi, M. and W. Leggate, *Investigating the effects of moisture ingress on the performance and service life of mass timber panels in Australian climates - Experimental testing plan* Q.G. Department of Agriculture and Fisheries, Editor. 2020.
- [9] Gereke, T., *Moisture-induced stresses in cross-laminated wood panels*. 2009, Dipl.-Ing., University of Leipzig.
- [10] Gereke, T., P. Hass, and P. Niemz, *Moisture-induced stresses and distortions in spruce cross-laminates and composite laminates*. Holzforschung, 2010. **64**(1): p. 127-133.
- [11] Gereke, T., et al., *Experimental and numerical determination of the hygroscopic warping of cross-laminated solid wood panels*. Holzforschung, 2009. **63**(3): p. 340-347.
- [12] Gereke, T., et al., *Identification of moisture-induced stresses in cross-laminated wood panels from beech wood (Fagus sylvatica L.)*. Wood science and technology, 2009. **43**(3-4): p. 301.
- [13] Taghiyari, H.R. and S. Avramidis, *Specific gas permeability of normal and nanosilver-impregnated solid wood species as influenced by*

- heat-treatment*. Maderas. Ciencia y tecnología, 2019. **21**(1): p. 89-96.
- [14] Redman, A., et al., *Mass transfer properties (permeability and mass diffusivity) of four Australian hardwood species*. BioResources, 2012. **7**(3): p. 3410-3424.
- [15] Redman, A., *Modelling of vacuum drying of Australian hardwood species*. 2017, Queensland University of Technology.
- [16] Popper, R., P. Niemz, and S. Croptier, *Adsorption and desorption measurements on selected exotic wood species: Analysis with the Hailwood-Horrobin model to describe the sorption hysteresis*. Wood research, 2009. **54**.
- [17] Jang, E.-S., J.-H. Yuk, and C.-W. Kang, *An experimental study on change of gas permeability depending on pore structures in three species (hinoki, Douglas fir, and hemlock) of softwood*. Journal of Wood Science, 2020. **66**(1): p. 1-12.
- [18] Kukk, V., et al., *Designing highly insulated cross-laminated timber external walls in terms of hygrothermal performance: Field measurements and simulations*. Building and Environment, 2022. **212**: p. 108805.
- [19] Chang, S.J., et al., *Assessment of effect of climate change on hygrothermal performance of cross-laminated timber building envelope with modular construction*. Case Studies in Thermal Engineering, 2021. **28**: p. 101703.
- [20] Schiavoni, S., F. Bianchi, and F. Asdrubali, *Insulation materials for the building sector: A review and comparative analysis*. Renewable and Sustainable Energy Reviews, 2016. **62**: p. 988-1011.
- [21] Balaji, N., M. Mani, and B.V. Reddy, *Discerning heat transfer in building materials*. Energy Procedia, 2014. **54**: p. 654-668.
- [22] Leggate, W., et al., *Influence of Wood's Anatomical and Resin Traits on the Radial Permeability of the Hybrid Pine (Pinus elliottii × Pinus caribaea) Wood in Australia*. BioResources, 2020. **15**(3): p. 6851-6873.
- [23] Schmidt, E.L., et al., *Environmental response of a CLT floor panel: Lessons for moisture management and monitoring of mass timber buildings*. Building and Environment, 2019. **148**: p. 609-622.
- [24] Quesada-Pineda, H., et al., *A Visual Assessment of Cross-laminated Timber Structures in Austria*. BioProducts Business, 2020: p. 51-62.
- [25] MacKenzie, C., et al., *Timber Service Life Design Guide*. 2007, Forest & Wood Products Australia Limited.
- [26] Bucklin, O., et al., *Mono-material wood wall: Novel building envelope using subtractive manufacturing of timber profiles to improve thermal performance and airtightness of solid wood construction*. Energy and Buildings, 2022. **254**: p. 111597.
- [27] Beebe, K. and M. Kam-Biron, *five Ds of moisture management: deflection, drainage, drying, distance and durable materials in SEAOC 2016*. 2016. p. 18.
- [28] Niklewski, J., et al., *Moisture conditions of rain-exposed glue-laminated timber members: the effect of different detailing*. Wood Material Science & Engineering, 2018. **13**(3): p. 129-140.
- [29] Franke, B., et al. *Moisture diffusion in wood—Experimental and numerical investigations*. in *CD-ROM Proceedings of the World Conference on Timber Engineering*. 2016.
- [30] RuthMcClung, et al., *Hygrothermal performance of cross-laminated timber wall assemblies with built-in moisture: field measurements and simulations*. Building and Environment, 2014. **71**(January 2014): p. 95-110.
- [31] *Wood Reference Collection*. Department of Agriculture and Fisheries Queensland Government.
- [32] Manh, H.T., et al., *Mass transfer properties of Acacia mangium plantation wood*. Maderas. Ciencia y tecnología, 2022. **24**.
- [33] Cai, C., et al., *Effect of natural weathering on water absorption and pore size distribution in thermally modified wood determined by nuclear magnetic resonance*. Cellulose, 2020. **27**(8): p. 4235-4247.
- [34] Peng, L.M., et al., *Analysis of wood pore characteristics with mercury intrusion porosimetry and X-ray micro-computed tomography*. Wood research, 2015. **60**(6): p. 857-864.
- [35] Zauer, M., A. Pfriem, and A. Wagenführ, *Toward improved understanding of the cell-wall density and porosity of wood determined by gas pycnometry*. Wood science and technology, 2013. **47**(6): p. 1197-1211.
- [36] Friquin, K.L., *Material properties and external factors influencing the charring rate of solid wood and glue-laminated timber*. Fire and materials, 2011. **35**(5): p. 303-327.
- [37] De Ligne, L., et al., *Moisture dynamics of wood-based panels and wood fibre insulation materials*. Frontiers in Plant Science, 2022. **13**.
- [38] Plötze, M. and P. Niemz, *Porosity and pore size distribution of different wood types as determined by mercury intrusion porosimetry*. European journal of wood and wood products, 2011. **69**(4): p. 649-657.
- [39] Sarkar, K. and B. Bhattacharjee, *Modeling of tropical rainfall exposure for the study of moisture penetration in porous building materials*. Journal of Hydrologic Engineering, 2017. **22**(8): p. 04017017.

- [40] Bobadilha, G.d.S., et al., *Physical, optical, and visual performance of coated cross-laminated timber during natural and artificial weathering*. *Coatings*, 2021. **11**(2): p. 252.
- [41] Redman, A.L., et al., *Characterisation of wood–water relationships and transverse anatomy and their relationship to drying degrade*. *Wood Science and Technology*, 2016. **50**: p. 739-757.